Point Cloud Segmentation with LIDAR Reflection Intensity Behavior

Akin Tatoglu & Kishore Pochiraju

***Abstract*— Light Detection and Ranging (LIDAR) scans are increasingly being used for 3D map construction and reverse engineering. The utility and benefit of the processed data maybe enhanced if the objects and geometry of the area scanned can be segmented and labeled. In this paper, we present techniques to model the intensity of the laser reflection return from a point during LIDAR scanning to determine diffuse and specular reflection properties of the scanned surface. Using several illumination models, the reflection properties of the surface are characterized by Lambertian diffuse reflection model and Blinn-Phong, Gaussian and Beckmann specular models. Experimental set up with eight different surfaces with varied textures and glossiness enabled measurement of algorithm performance. Examples of point cloud segmentation with the presented approach are presented.**

I. Introduction

POINT clouds generated using Light Detection and Ranging (LIDAR) systems can cover large areas and contain many details. [1],[2]. Identification and delineation (segmentation of the image or point cloud) of various objects in the point data is of significant consequence to various downstream applications. For example, an autonomous mobile robot working in an unstructured environment can identify objects of interest as well as their location and sizes. Classification of terrains generated from equipment mounted on planes into forests, desert, and wetlands enable quick mapping of physical features. Some research exists for extracting surface features, terrain classification and obstacle detection using Gabor filter banks and using LIDAR data to perceive the difference between obstacle and other vegetative objects (i.e. rock and grass.) [3], [4], [10]

Applying segmentation algorithms to locate and label objects in an environment may be crucial in many tasks. Analyzing objects in an environment only from geometrical point of view could not be sufficient. Compliant foliage and brush may be geometrically considered as an obstacle however an autonomous ground vehicle could safely drive over it [10]. Shiny objects like mirrors reflects the light on unpredicted directions and cause noise in LIDAR ranging data and camera image data[5]. There are several current methods to segment attributes from point clouds from a geometrical point of view [2], [6].

Akin Tatoglu is a doctoral student and a research assistant in the Department of Mechanical Engineering Stevens Institute of Technology, Hoboken, NJ 07030 (Phone: 201-216-8215; fax: 201- 216-8963; e-mail: atatoglu@ stevens.edu).

Dr. Kishore Pochiraju is an Associate Professor in Mechanical Engineering and the director of the Design & Manufacturing Institute at Stevens Institute of Technology, Hoboken, NJ 07030.

In prior efforts, aerial vehicle and satellite reflectance data were used to define a bidirectional distribution function. This function was utilized to determine the type of the terrain surface and albedo values of surfaces under different weather and seasonal conditions. As a result, terrain surfaces were classified as forest, desert, wetland etc. [6].

Use of reflection intensity which is generally available from many LIDAR ranging devices may assist in the segmentation and labeling task. The behavior of the light propagation could be listed as refraction, reflectance, absorption, scattering, and polarization [7]. The reflected light from incident laser light is sensed in a LIDAR. Reflectance measures the ratio of amount of radiation sent to the material surface over the amount received by the LIDAR equipment. Utilizing reflection intensity maps to segment materials or structures could improve the overall performance of different types of applications including automatic cruise control, agricultural analysis, weather analysis, hazardous area analysis, terrain type detection etc [8],[9],[10]. However, the reflection intensity depends upon several factors including the distance to the object, view angle and the surface characteristics.

In this paper, we explore the use of illumination models derived from computer graphics to characterize the LIDAR reflection intensity data. Lambertian diffuse reflection [11] along with Blinn-Phong [12], Gaussian [13] and Beckmann [14] specular reflection models were used to characterize the reflection characteristics of the underlying scanned surface. The diffuse reflection coefficient is shown to be useful for segmenting large point clouds.

II. LIDAR Reflection Return Models

Many time of flight LIDAR scanners provide the laser reflection intensity observed by the photo-detector. The intensity of reflection return depends, in general, upon the distance to the object, the angle between the surface normal and the incident laser ray and the glossiness of the surface. We examine the reflection intensity data in a typical 3D point cloud to characterize the diffuse and specular reflectivity characteristics of the scanned surface. In computer graphics applications where realistic shading of synthetic surfaces is desired, models such as the Blinn-Phong [12], Gaussian [13] and Beckmann [14] are often used for rendering surfaces. These models employ parameters depicting the material behavior. The main hypothesis of this paper is to characterize a set of "best-fit" parameters that represent the scanned surface and use the

parameter set as the attributes in a segmentation algorithm. Both spatial and reflection property similarities in the point cloud enable segmentation of the point cloud and potentially labeling after suitable comparison with known material signatures. The point-light source surface illumination model of particular interest in this context.

In this analysis we consider Blinn-Phong [12] model for analysis that incorporates both the Lambertian (diffuse) and specular reflection components as well as Gaussian [13] and Beckmann [14] models to model specular reflection properties on textured surfaces. The Lambertian reflection model defines the diffuse reflection for the dull, matte surfaces. The amount of intensity reflected by these types of materials is independent of the relationship between the view angle and the surface normal. We model the reflection intensity model for single wavelength incident ray with diffuse and specular components as given in (1).

$$\mathrm{R} = \frac{I_\lambda}{I_{p\lambda}} = Z_{att}\,[k_d cos\theta + \mathrm{k_s}] \tag{1}$$

We define the R as the ratio of the reflected to incident intensities of the light at a frequency λ. As the incident ray cast by the LIDAR is typically tuned to a single infrared frequency and the output of the photo detector sensing the reflected ray is tuned to the same frequency, the scalar R is assumed as the measurement obtained from the LIDAR as the reflection intensity of the return. The measurement is normalized on a 0 - 1 scale. Z_{att} denotes the attenuation of the reflection intensity due to the distance between the LIDAR and scanned surface. The divergence in the incident beam causes substantial range dependent attenuation

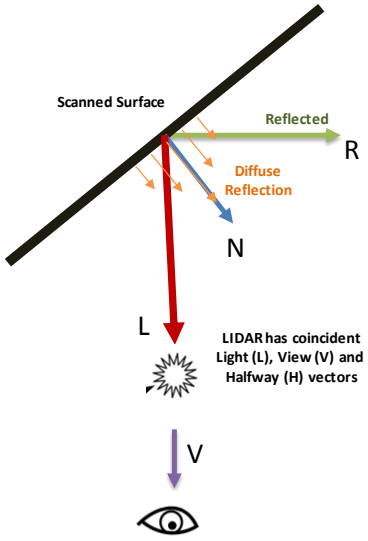

Fig. 1. Incident and reflected rays during LIDAR ranging. Rough surfaces may have local variations in the normal vector leading to loss in reflection intensity

We adopted three models to characterize the specular reflection characteristics of the scanned materials. First we used the Blinn-Phong model for which the specular reflection component k_s is given in (2). The model requires two parameters, k^{BP} and exponent, n.

$$\mathrm{R} = \frac{I_\lambda}{I_{p\lambda}} = Z_{att}\,[k_d cos\theta + \mathrm{k^{BP}}\cos^{\mathrm{n}}\alpha] \tag{2}$$

Blinn-Phong model uses the half way vector, H, which is defined as the mean of light and view vectors [15]. In the case of a LIDAR, L and V are nearly coincident and hence L = H = V. Therefore, for this case Cosα = N.H = N.L. Therefore, the Blinn-Phong and Phong models produce identical results for this case.

$$H = \frac{L+V}{|\,L+V\,|} = L \tag{3}$$

Gaussian and Beckmann models consider the local surface texture using a micro-facet analogy. The Gaussian distribution defines the specular reflection as in (4). One parameter, m∈ {0, 1}, represents the texture characteristics. The specular reflection component for the Beckmann distribution is shown in (9). This model also requires one parameter, B, to describe the texture of the material.

$$k_{s\,[Gaussian]} = e^{-(\frac{\beta}{m})^2} \tag{4}$$

$$k_{s\,[Beckman]} = \frac{\exp\left(-\frac{tan^2(\beta)}{B^2}\right)}{\pi B^2 cos^4(\beta)} \qquad \beta = \arccos(N,H) \tag{5}$$

III. Experimental Material Characterization

An image-registered 2D LIDAR system [10] mounted on a rotating frame was used to generate point clouds of several materials with varying texture and reflectivity. The scanning system generated the coordinate, color information and reflection intensity as {X, Y, Z, I, R, G, B} at each scanning point. The LIDAR used for this analysis was a SICK LMS-200 and a camera with 1280x960 resolution is registered to the scanning plane. The LIDAR generated {X, Y, Z, I} data elements and the camera provided the corresponding {R, G, B} color data in real-time.

The experimental setup used included several material swatches (about 60 cm x 60 cm) in area were placed at various distances in front of the LIDAR and the point clouds were generated with reflection intensity and color information. The luminosity component from the {R,G,B} data was also analyzed but not presented in this paper as no correlation was detected between the laser reflectivity (905 nm infrared wavelength) and luminosity in the visible color spectrum.

In setup-1, three different materials were used and point clouds were generated at six distances - 1.6 m, 4 m, 6.4 m, 8m, 12m and 20m. The distance effects are measured by using a small target for which the view angle variation is minimal as shown in Fig. 2.

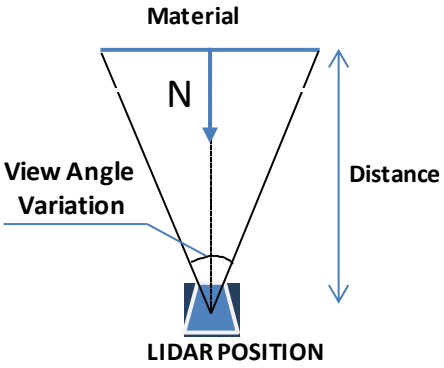

Fig. 2. In experimental setup-I, material swatches were placed directly in front of the LIDAR. The rotation of the scanning mirror causes the view angle (V.N) to change for various points on the surface. However, the variation of the view angle is small, about 2-3°.

A second experimental setup was used to study the effect of view angle. In this experiment, each material swatch is translated from the center of the LIDAR by known distances (D_x, D_y) and thereby varying the view angle from 0° to 40°. A distance of 6 m was used for position-A and the D_y value for position-E was 4.59m. At these distances, the effect of Z_{att} is assumed to be minimal due to the changes in the range.

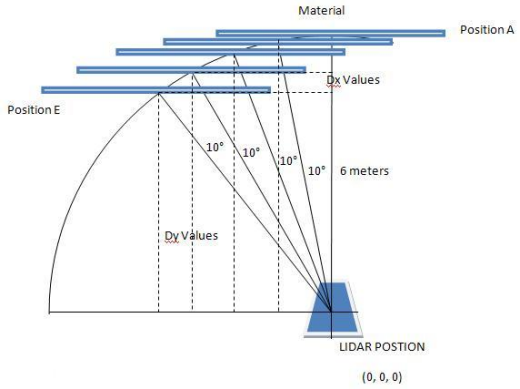

Fig. 3. In experimental setup-II, the view angle is varied considerably by repositioning the swatch.

IV. Characterization of Reflection Properties

Fig. 4 shows the intensity attenuation due to the distance between the LIDAR and the surface being scanned. This attenuation can be attributed to the beam divergence and the incident spot diameter grows with the distance from the scanner. The results in Fig. 4 can be used to determine Z_{att} in (2). The figure shows that between 4 and 8 meters the intensity decreases linearly.

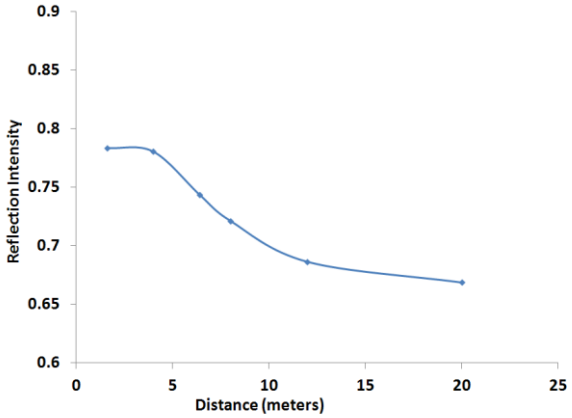

Fig. 4. Intensity dependence on the distance to the scanner

Aluminum (Al), Copper (Cu), Foam (grey and white), Steel and Wood swatches were placed at a nominal distance of 6m and reflection intensity values were obtained using the LIDAR. The reflection values for each of the material swatches were used to determine the best fit parameters for the Blinn-Phong, Gaussian and Beckmann models. Fig. 5 and 6 show the LIDAR reflection intensity measurements with view angle for Al and black foam sheets. Reflection intensity varies with the incident angle and considerable variability is also evident in the reflection intensity for points with the same view angle. While the coarse change in the intensity with view angle is expected for objects with specular reflection characteristics, the variability is attributed to the local surface normal changes in the thin aluminum sheet used for experimentation. Any aberration or imperfection changes the normal estimate and can lead to the variability in reflection intensity. The Gaussian and Beckmann models use a micro-facet analogy to account for such variations. Characterization of local surface normal variations may be important to properly characterize the reflection intensity. The black foam board used in Fig. 6 has smooth rigid surface with minimal surface distortions. The reflection intensity is lower for the board and no dependence is evident on the view angle indicating diffuse reflection.

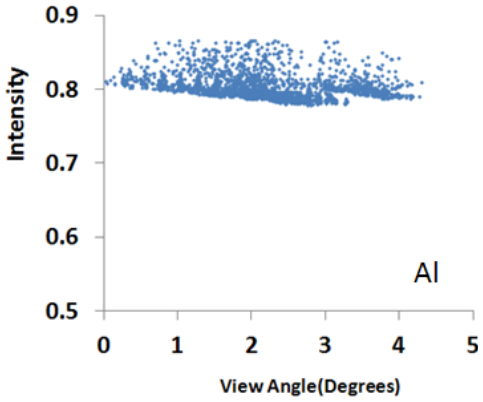

Fig. 5. Raw intensity data for Al swatch. Intensity variations are due to view angle changes and local surface normal variations.

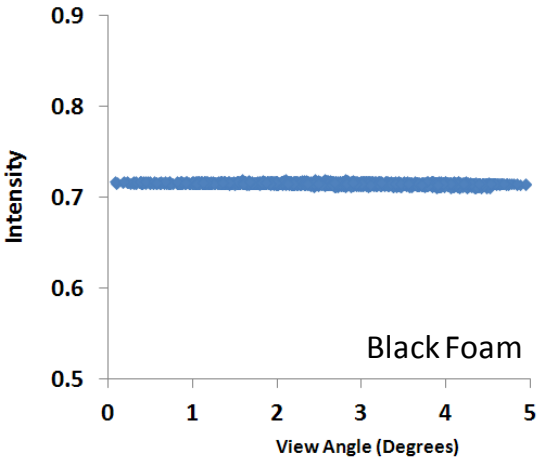

Fig. 6. Reflection intensity for a black foam board

Fig. 7 shows the diffuse reflection coefficients for various materials. The coefficient is relatively constant with the grey foam showing increased absorbance compared to the other materials. Fig. 8 shows coefficient values for K^{BP} in (2) and the shiny materials show higher coefficient than the dull materials as expected.

Experiment setup –II was used to determine the effect of view angle on the reflection intensity for Aluminum and black foam swatches. The view angle was varied from 0 to 45°. Fig. 9 shows the Beckmann and Gaussian model behavior in comparison with the experimental data. The blue discrete points represent the experimentally measured intensity response and the red line represents the Beckmann model with B = 300. The Gaussian model with m=0.04 is also shown. These two parameter values produced the best fit to the measured reflection intensity. No noise filtering was performed before plotting the experimental data. Both the models captured the view dependence qualitatively. However, the entire data set had to be used for finding the best fit parameters.

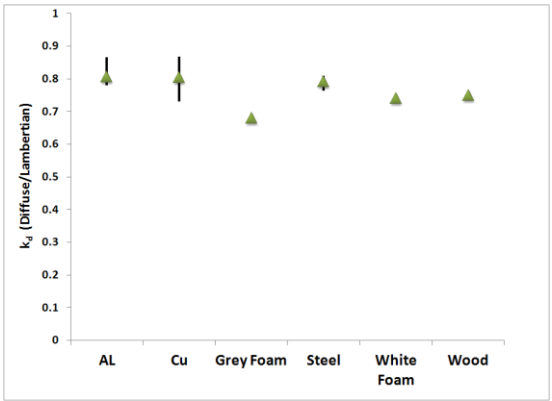

Fig. 7. Diffuse reflection coefficient K_d for 905 nm incident light for various materials.

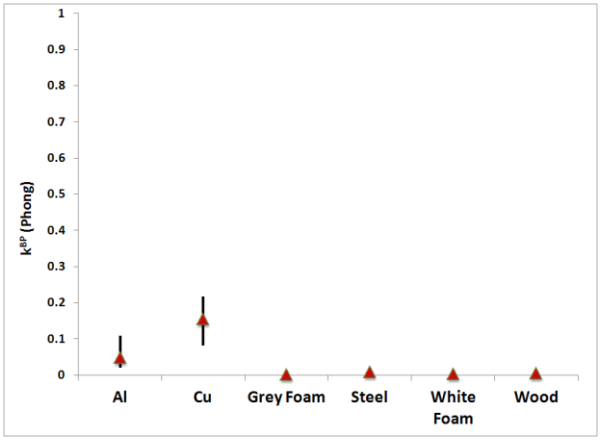

Fig. 8. Specular reflection coefficient KBP for various materials with n=2.

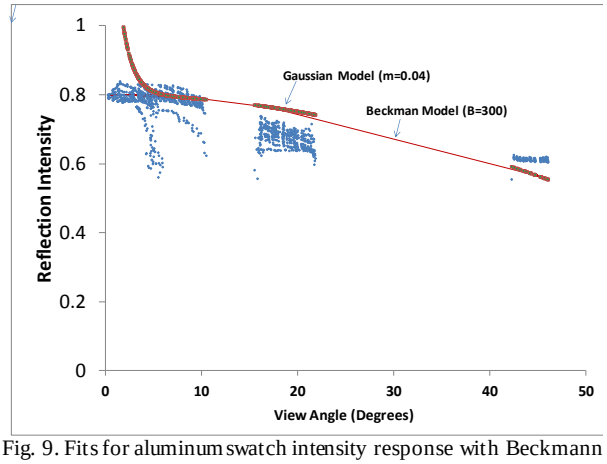

Fig. 9. Fits for aluminum swatch intensity response with Beckmann and Gaussian models

V. Segmentation of Point Clouds

In this section we consider a LIDAR scan of an outdoor scene. The point cloud with image registration and intensity data is shown in Fig. 10. The figure shows {x,y,z,r,g,b} data in an image format. The scene consists of a sculpture, its foundation and several landscape features. The ambient lighting substantially affects the quality of the image and details of the sculpture are barely discernable. Due to the time of the day, lighting is bright on the opposite side from the camera position shown in the figure.

The intensity data of the scene were processed for diffuse and specular reflection parameters in the Blinn-Phong model. The diffuse reflection coefficient K_d is computed and plotted for the entire scene using a color map. In this color scale, red denotes K_d=1 and blue K_d=0. Fig. 11 shows the map of the diffuse reflection coefficient K_d. The figure clearly delineates the sculpture from the scene. The reflection returns also shows several features (shrubs beneath the sculpture) under exposed in the camera image. Therefore the diffuse reflection component can potentially

be used to delineate features in point clouds that are otherwise obscured due to lighting conditions.

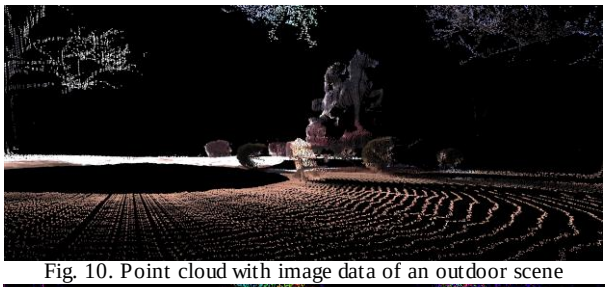

Fig. 10. Point cloud with image data of an outdoor scene

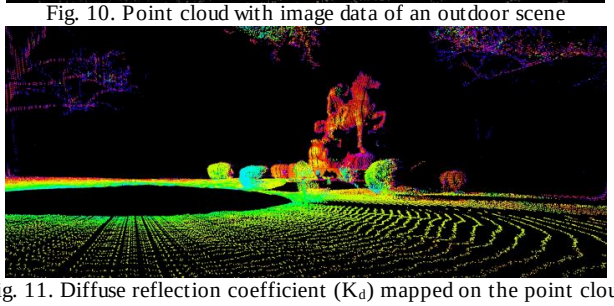

Fig. 11. Diffuse reflection coefficient (K_d) mapped on the point cloud

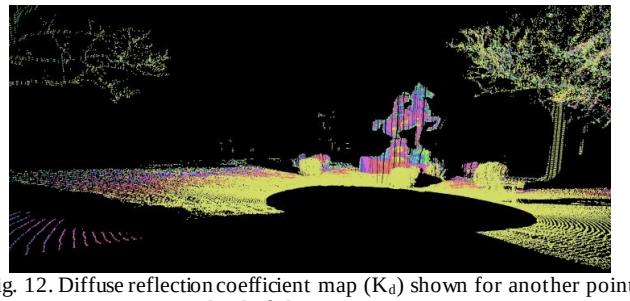

Fig. 12. Diffuse reflection coefficient map (K_d) shown for another point cloud of the same scene.

The LIDAR was moved to a second location and portions of the scene shown in Fig. 10 rescanned. The reflection intensity was again processed to determine K_d variation in the scene. Fig. 11 shows the map of the sculpture with the K_d values plotted as a color. Material reflection response was qualitatively similar between the two scans and the K_d values were similar.

A basic Receiver Operating Characteristic (ROC) analysis was conducted to evaluate the effectiveness of the classifier. Points are manually into positive (belongs to statue) and negative (doesn't belong to the statue) sets. The points analyzed were 99695 negative and 3736 positive. The points were then reclassified based on K_d. A mean value of K_d was computed for the positive set and True Positives, False Positives, True Negatives and False Negatives were determined based on the K_d distribution of the point set. Of the nearly 100,000 classified points, 69.8% were accurately classified and the sensitivity to True Positives was found to be 94.6%.

VI. CONCLUDING REMARKS

In the paper, we present a methodology for using the LIDAR reflection return values for segmenting point clouds based on the diffuse and specular reflection behavior. We performed several experiments to under the behavior various surfaces and the performance of the illumination models in characterizing the LIDAR reflection data. The paper shows the use of diffuse reflection coefficient K_d in a Lambertian reflection model as an attribute to segment point clouds. Work is in progress for determining the performance of specular reflection parameters. We are currently pursuing robust determination of surface normals from point cloud data, which leads to an accurate determination of the viewing angle for each point. We expect that the scatter in the measured reflection intensity vs. view angle response will decrease considerably with robust normal computation and leads to better characterization of specular reflection. The use of K_s may be appropriate when the scene contains several shiny objects. The variations in the diffuse reflection coefficient K_d may be adequate when the scene has several dull objects.

REFERENCES

[1] Gebre, B., Men, H and Pochiraju K., 2009, "Remotely Operated and Autonomous Mapping System (ROAMS)," IEEE International Conference on Technologies for Practical Robot Applications, IEEE, pp. 173-178.

[2] Cole D. M., and Newman P. M., 2006, "Using laser range data for 3D SLAM in outdoor environments," Robotics and Automation, 2006. ICRA 2006. Proceedings 2006 IEEE International Conference on, IEEE, p. 1556–1563.

[3] Castano R., Manduchi R., and Fox J., 2001, "Classification experiments on real-world texture," Third Workshop on Empirical Evaluation Methods in Computer Vision, Kauai, Hawaii, December 10, 2001., Pasadena, CA: Jet Propulsion Laboratory, National Aeronautics and Space Administration,.

[4] Hautecœur O., and Leroy M. M., 1998, "Surface bidirectional reflectance distribution function observed at global scale by POLDER/ADEOS," Geophysical Research Letters, 25(22), p. 4197.

[5] Yang S. W., and Wang C. C., 2011, "On Solving Mirror Reflection in LIDAR Sensing," Mechatronics, IEEE/ASME Transactions on, 16(99), p. 1–11.

[6] Vandapel N., and Hebert M., "Finding organized structures in 3-D ladar data," 2004 IEEE/RSJ International Conference on Intelligent Robots and Systems (IROS) (IEEE Cat. No.04CH37566), pp. 786-791.

[7] Richmond, Richard D., and Stephen C. Cain. 2010. Direct-detection LADAR systems. SPIE Press. Bellingham, Wash.

[8] Lindner P., Richter E., and Wanielik G., 2009, "Multi-Channel Lidar Processing for Lane Detection and Estimation," October, pp. 202-207.

[9] Saeys W., Lenaerts B., Craessaerts G., and Debaerdemaeker J., 2009, "Estimation of the crop density of small grains using LiDAR sensors," Biosystems Engineering, 102(1), pp. 22-30.

[10] Manduchi R., Castano a, Talukder a, and Matthies L., 2005, "Obstacle Detection and Terrain Classification for Autonomous Off-Road Navigation," Autonomous Robots, 18(1), pp. 81-102.

[11] J. Lambert, 1760, "Photometria Sive de Mensura et Gradibus Luminus, Colorum et Umbrae," Eberhard Klett .

[12] Blinn J. F., 1977, "Models of light reflection for computer synthesized pictures," Proceedings of the 4th annual conference on Computer graphics and interactive techniques, ACM, p. 192–198.

[13] Sparrow E. M., Torrance K. E., Sparrow E. M., and Birkebak R. C., 1967, "Theory for Off-Specular Reflection From Roughened Surfaces," Journal of the Optical Society of America, 57(9).

[14] Beckmann, P., 1963, "The scattering of electromagnetic waves from rough surfaces", Pergamon Press, NY

[15] Foley J. D., van Dam A., Feiner S. K. and Hughes J. F., 1997, "Computer Graphics: Principles and Practice Second Edition", C. Addison Wesley